

Weighted medical image registration with automatic mask generation

Hanno Schumacher^a, Astrid Franz^b, Bernd Fischer^a

^aInstitute of Mathematics, University of Lübeck, Wallstrasse 40, 23560 Lübeck, Germany

^bPhilips Research Laboratories, Röntgenstrasse 24-26, 22335 Hamburg, Germany

ABSTRACT

Registration of images is a crucial part of many medical imaging tasks. The problem is to find a transformation which aligns two given images. The resulting displacement fields may be for example described as a linear combination of pre-selected basis functions (parametric approach), or, as in our case, they may be computed as the solution of an associated partial differential equation (non-parametric approach). Here, the underlying functional consists of a smoothness term ensuring that the transformation is anatomically meaningful and a distance term describing the similarity between the two images. To be successful, the registration scheme has to be tuned for the problem under consideration. One way of incorporating user knowledge is the employment of weighting masks into the distance measure, and thereby enhancing or hiding dedicated image parts. In general, these masks are based on a given segmentation of both images. We present a method which generates a weighting mask for the second image, given the mask for the first image. The scheme is based on active contours and makes use of a gradient vector flow method. As an example application, we consider the registration of abdominal computer tomography (CT) images used for radiation therapy. The reference image is acquired well ahead of time and is used for setting up the radiation plan. The second image is taken just before the treatment and its processing is time-critical. We show that the proposed automatic mask generation scheme yields similar results as compared to the approach based on a pre-segmentation of both images. Hence for time-critical applications, as intra-surgery registration, we are able to significantly speed up the computation by avoiding a pre-segmentation of the second image.

Keywords: registration, weighted distance measures, weighting masks, segmentation, active contours

1. INTRODUCTION

Medical image registration is still one of today's most challenging imaging problems. The images may have been acquired with the same or different imaging modalities, simultaneously or at different times, or from one or several patients. In order to compare the images, it is important to know, how corresponding structures were shifted and deformed. The calculation of this displacement is the aim of image registration (see¹⁻⁴ and references therein). The displacement field may be described as a linear combination of pre-selected basis functions (parametric approach) or, as in our case, they may be computed as the solution of an associated partial differential equation, known as variational approach or parameter-free registration approach.¹ Here, one minimizes the functional

$$J(\mathbf{u}; \mathbf{R}, \mathbf{T}) = \alpha \cdot S(\mathbf{u}) + D(\mathbf{u}; \mathbf{R}, \mathbf{T}), \quad (1)$$

where \mathbf{u} is the sought displacement field, \mathbf{R} is the reference image, which stays fixed during the registration process, \mathbf{T} is the template image, which will be transformed, S is a smoother ensuring that the displacement field satisfies certain smoothness constraints, D a distance measure measuring the similarity of the two images, and α a regularization parameter tuning the influence of S and D . In the literature, one may find a wide range of different choices for S and D . Widely used smoother include the so-called diffusive,⁵ elastic,^{6,7} and the curvature functional,⁸ respectively. This paper is based on the elastic smoother

$$S(\mathbf{u}) = \int_{\Omega} \frac{\mu}{4} \sum_{j,k=1}^2 (\partial_j u_k(\mathbf{x}) + \partial_k u_j(\mathbf{x}))^2 + \frac{\lambda}{2} (\operatorname{div} \mathbf{u}(\mathbf{x}))^2 \mathrm{d}\mathbf{x}$$

with the material dependent Lamé constants λ and μ and the region of interest Ω . Our choice for the elastic smoother is motivated by the fact that it mimics the elastic behavior of soft tissue. However, the developed techniques are applicable to any other smoother as well. Popular distance measures include the sum of squared grey value differences (SSD), the mutual information (MI)^{9, 10} or the cross correlation (CC).¹¹ For the ease of presentation, we restrict ourselves to the SSD measure.

Sometimes it is desirable to supplement the distance measures by certain weighting strategies. Such a weighting scheme may be used to suppress irrelevant image structures like different rectum fillings in abdominal CT images, as such a situation would trap any registration procedure. Or the weighting approach may be used to enhance the contrast between different tissue types with very similar grey values, which are otherwise hard to detect.

The drawback of a weighting scheme, however, is the need of a sound segmentation of the critical areas in both images. Segmentation is a computationally expensive task. The present paper was driven by a radiation therapy application. Here, one image is taken well in advance of the actual therapy. Consequently, a detailed segmentation of this template image is feasible. On the other hand, the second image is taken just before the therapy and has to be processed in nearly real-time. Hence one may want to avoid a time-consuming segmentation step for this reference image.

It is the goal of this paper to present a method for creating the needed weighting mask for the reference image. To generate the reference mask the known mask of the template image is deformed accordingly. Therefore, the new approach opens the door for time critical weighted registration tasks.

The paper is organized as follows. Section 2 starts with a short summary of the weighted registration methodology. This is followed by detailed description on how one may calculate the mask for the reference image, given the mask for the template image. The main ingredient is a gradient vector flow based snake algorithm. Section 3 compares the new method with a weighted registration scheme based on given masks for both the reference and template image. Academic image sets as well as real-life CT image sets are presented. Finally, some conclusions are drawn in Section 4.

2. METHOD

2.1. Weighted non-linear image registration

Given a reference image \mathbf{R} and a template image \mathbf{T} , to be transformed, we search for a displacement field \mathbf{u} that minimizes the functional (1). Throughout this paper we consider the SSD distance measure

$$D(\mathbf{u}; \mathbf{R}, \mathbf{T}) = \frac{1}{2} \int_{\Omega} (\mathbf{T}(\mathbf{x} - \mathbf{u}(\mathbf{x})) - \mathbf{R}(\mathbf{x}))^2 dx.$$

In order to enhance important image structures and/or to suppress irrelevant image parts, weighting masks may be incorporated into the distance measure, like

$$D(\mathbf{R}, \mathbf{T}, \mathbf{M}_{\mathbf{R}}, \mathbf{M}_{\mathbf{T}}; \mathbf{u}) = \frac{1}{2} \int_{\Omega} [(\mathbf{T}(\mathbf{x} - \mathbf{u}(\mathbf{x})) - \mathbf{R}(\mathbf{x})) \cdot (\mathbf{M}_{\mathbf{T}}(\mathbf{x} - \mathbf{u}(\mathbf{x})) - \mathbf{M}_{\mathbf{R}}(\mathbf{x})) \cdot \mathbf{M}_{\mathbf{A}}(x)]^2 dx, \quad (2)$$

called SSD^{mix} , since it is a mixture of an additive and a multiplicative weighting.¹² The definition of the reference mask $\mathbf{M}_{\mathbf{R}}$, the template mask $\mathbf{M}_{\mathbf{T}}$ and the third mask $\mathbf{M}_{\mathbf{A}}$ are as follows. Let $B_T^{(i)}, B_R^{(i)} \subset \Omega, i = 1, 2, \dots, m$ denote the corresponding problematic areas of \mathbf{T} and \mathbf{R} , respectively. It is assumed that these subsets are simply connected, closed, and mutually distinct, i.e., $B_T^{(i)} \cap B_R^{(j)} = \emptyset$ for $i \neq j$. Furthermore, let $b_i \in \mathbb{R}^+$ denote the

weighting factor for $B_T^{(i)}$ and $B_R^{(i)}$, respectively. Then we define

$$\begin{aligned} \mathbf{M}_T(\mathbf{x}) &= \begin{cases} b_i & : \mathbf{x} \in B_T^{(i)} \\ 1 & : \text{otherwise} \end{cases}, \\ \mathbf{M}_R(\mathbf{x}) &= \begin{cases} b_i + 1 & : \mathbf{x} \in B_R^{(i)} \\ 0 & : \text{otherwise} \end{cases}, \\ \mathbf{M}_A(\mathbf{x}) &= \begin{cases} 0 & : \mathbf{x} \in B_R^{(i)} \wedge b_i = 0 \\ 1 & : \text{otherwise} \end{cases}. \end{aligned}$$

Consequently, the difference image $\mathbf{T}(\mathbf{x} - \mathbf{u}(\mathbf{x})) - \mathbf{R}(\mathbf{x})$ is multiplied by -1 for $\mathbf{x} \in B_R^{(i)} \wedge \mathbf{x} \in B_T^{(i)}$, by b_i for $\mathbf{x} \notin B_R^{(i)} \wedge \mathbf{x} \in B_T^{(i)}$, and by $-b_i$ for $\mathbf{x} \in B_R^{(i)} \wedge \mathbf{x} \notin B_T^{(i)}$. The additional mask \mathbf{M}_A is needed to suppress an unwanted area for the case $B_R^{(i)} \cap B_T^{(i)} \neq \emptyset$.

The distance measure with weights (2) leads to the modified functional

$$J(\mathbf{u}; \mathbf{R}, \mathbf{T}, \mathbf{M}_R, \mathbf{M}_T) = \alpha \cdot S(\mathbf{u}) + D(\mathbf{R}, \mathbf{T}, \mathbf{M}_R, \mathbf{M}_T; \mathbf{u}) \quad (3)$$

which has to be minimized with respect to the displacement field \mathbf{u} . To obtain a necessary condition for a minimizer, the Gâteaux derivative of the functional (3) is computed. The derivative of the new distance measure looks like

$$\begin{aligned} \mathbf{f}(\mathbf{x}, \mathbf{u}(\mathbf{x})) &= -\mathbf{M}_A(\mathbf{x})^2 \cdot [(\mathbf{T}(\varphi(\mathbf{x})) - \mathbf{R}(\mathbf{x})) \cdot (\mathbf{M}_T(\varphi(\mathbf{x})) - \mathbf{M}_R(\mathbf{x}))] \\ &\quad \cdot [\nabla \mathbf{T}(\varphi(\mathbf{x})) \cdot (\mathbf{M}_T(\varphi(\mathbf{x})) - \mathbf{M}_R(\mathbf{x})) + \nabla \mathbf{M}_T(\varphi(\mathbf{x})) \cdot (\mathbf{T}(\varphi(\mathbf{x})) - \mathbf{R}(\mathbf{x}))], \end{aligned} \quad (4)$$

where $\varphi(\mathbf{x}) = \mathbf{x} - \mathbf{u}(\mathbf{x})$. The function \mathbf{f} is often called the force of the registration and drives the registration process.

This in turn leads to a partial differential equation, which is subsequently discretized by finite differences yielding a linear system of equations

$$\mathbf{A}\mathbf{u} = \mathbf{f}. \quad (5)$$

Here it is important to note that the matrix \mathbf{A} is connected to the smoother S , whereas the force vector \mathbf{f} , derived from (4), depends on the distance measure D only. Hence, changing the distance measure D only alters the right-hand side of equation (5), thus all known fast algorithms^{5,8,13,14} for solving (5) may still be employed.

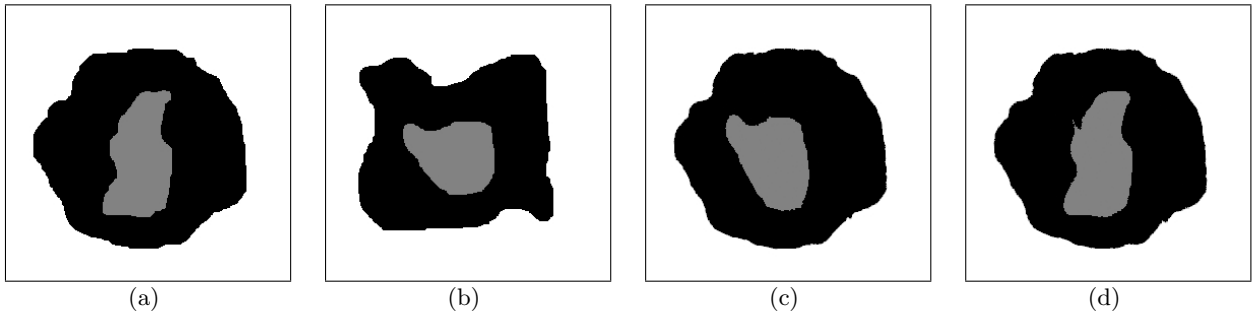


Figure 1. (a) reference image, (b) template image, (c) result of an elastic registration with distance measure SSD, (d) result of an elastic registration with distance measure SSD^{mix} .

Incorporating weighting masks into the similarity measure alters the force vector \mathbf{f} driving the registration. A clever choice does have a great impact on the registration result. To demonstrate this statement, we first consider an academic example. Figure 1a displays the reference and Figure 1b the template image, respectively. Note that the inner grey structure has a grey value of 245, the outer black structure of 255 and the white background

has grey value 0. Hence, the grey value difference between the inner and the outer structure is negligible as compared to the grey value difference between the outer structure and the image background. Therefore an unweighted registration is driven by the forces on the borders of the outer structure only and does not calculate an incomplete deformation field (see Figure 1c). Note, that the outer structure is nicely registered, whereas the inner structure is poorly registered. A weighted registration with the new distance measure SSD^{mix} , enhancing the inner structure by a weighting factor of 20, is able of calculating an almost perfect result (see Figure 1d).

2.2. Automatic generation of the reference mask

An obvious drawback of the weighted registration is the need for weighting masks in both images. To overcome this problem, an approach using only one mask is presented. The second mask is constructed automatically based on information obtained from the first mask. Consequently, the time consuming computation of the second mask is no longer necessary. To set up notation, we assume that the mask for the template is given and that the mask for the reference has to be constructed.

The computation of the second mask is based on a snake segmentation scheme. In order to successfully apply such a scheme, a 'good' starting contour is needed. Here, the necessary information is acquired from the given template mask by the following heuristic. First of all, the location of the template mask is used for getting a rough idea for a possible location of the mask in the reference image (see Figure 2a). Next, for the mask area in the template image an average grey value and its variance is calculated. The idea is, that apart from noise, the wanted area in the reference image will have similar grey values, as in our application the images are taken from one patient with the same scanner. The computed quantities are used to refine the initial mask approximation. More precisely, for every voxel within the initial mask of the reference image, it is checked whether its grey values fits within the interval given by the average grey value and the variance (compare, Figure 2b). Note that unwanted structures like a different rectum filling, will clearly not satisfy this grey value criterium. However, as long as these structures are within the interior of the wanted mask, this does not have any influence on our scheme (compare Figure 6). Finally, the surrounding contour is computed and used as start-contour for the snake based segmentation scheme (compare, Figure 2c).

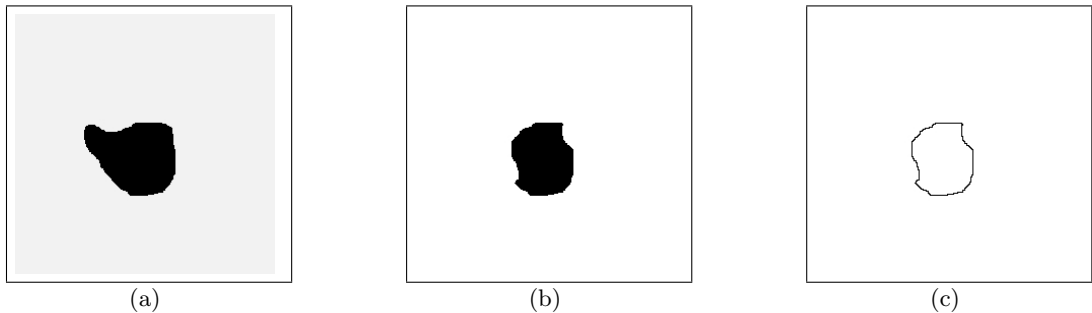


Figure 2. (a) template mask, (b) refined mask by using moments, (c) start contour for the snake scheme. Masks were obtained for the images shown in Figure 1a,b.

Next, the computed start-contour will be further refined by means of a snake based segmentation scheme. In the literature one may find a variety of snake approaches. Here, we use an active contour model¹⁵ which, in accordance with our registration scheme, may be seen as a variational problem, namely the minimization of the functional

$$E(\mathbf{v}) = \int_0^1 \frac{1}{2} [\beta \|\mathbf{v}'(s)\|_2^2 + \gamma \|\mathbf{v}''(s)\|_2^2] + \mathbf{E}_{\text{ext}}(\mathbf{v}(s)) \, ds. \quad (6)$$

Here, $v : [0, 1] \rightarrow \mathbb{R}^2$ is a parametric formulation of the wanted contour. Furthermore, the parameters β and γ may be used to tune the smoothness and flexibility of the contour. The term \mathbf{E}_{ext} represents the so-called external energy and does depend on the image under investigation.

A necessary condition for a minimizer v of the functional $E(\mathbf{v})$ is given by the Euler-Lagrange equation

$$-\beta \mathbf{v}''(s) + \gamma \mathbf{v}''''(s) + \nabla \mathbf{E}_{\text{ext}}(\mathbf{v}(s)) = 0, \quad (7)$$

supplemented by appropriate boundary conditions. It remains to choose an image dependent external energy. The idea is to base this energy on the edges \mathbf{B} of the reference image. To compute only relevant edges, an appropriate filter has to be applied. In general, a clever automatic choice of the filter is a tricky problem. Here, we make again use of the knowledge of the template image. Assuming that this image is corrupted by a similar noise, we learn from the template image, well ahead of time, on what is a successful filter (compare Figure 3).

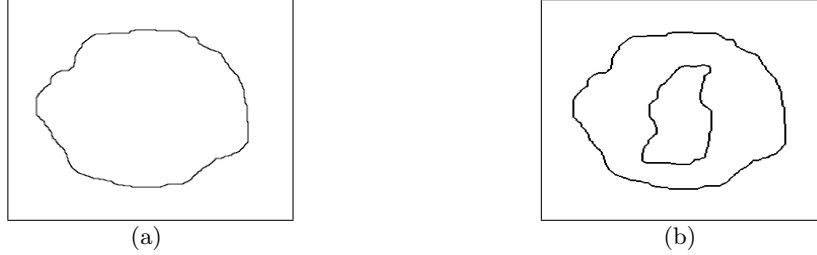


Figure 3. Edge-images \mathbf{B} of the reference image in Figure 1(a). (a) no pre-processing, (b) threshold based on the statistics of the template image.

Having computed an edge image \mathbf{B} , we employ the so-called gradient vector flow approach¹⁶ (GVF), which has been proven to be very successful. A GVF may be seen as a diffusive process applied to the edge image. It is defined by the functional

$$E(\mathbf{w}(\mathbf{x})) = \frac{1}{2} \int_{\Omega} \hat{\mu} (\|\partial_1 \mathbf{w}(\mathbf{x})\|_2^2 + \|\partial_2 \mathbf{w}(\mathbf{x})\|_2^2) + \|\nabla \mathbf{B}(\mathbf{x})\|_2^2 \|\mathbf{w}(\mathbf{x}) - \nabla \mathbf{B}(\mathbf{x})\|_2^2 \, d\mathbf{x} \quad (8)$$

Its minimization does produce a vector-field \mathbf{w} which is close to $\nabla \mathbf{B}$ at edges and smooth in the rest of the domain. This process may be tuned by the regularization parameter $\hat{\mu}$. Again, we apply the calculus of variations and obtain the Euler-Lagrange equation

$$\hat{\mu} \Delta \mathbf{w}(\mathbf{x}) - (\mathbf{w}(\mathbf{x}) - \nabla \mathbf{B}(\mathbf{x})) \|\nabla \mathbf{B}(\mathbf{x})\|_2^2 = 0 \quad (9)$$

with appropriate boundary conditions.



Figure 4. (a) start contour, (b) contour obtained by the GVF approach.

The snake-based segmentation scheme is illustrated in Figure 4. It shows the start contour and the result obtained by the snake scheme.

3. RESULTS

To validate the performance of the proposed approach, a weighted registration with two given masks is compared to a weighted registration where only the template mask is given. We start out with the academic example (see

Figure 1) and move on to real life example given by abdominal CT images recorded from the same patient at different times.

The registration schemes are based on an elastic smoother⁶ and the SSD^{mix} distance measure. To bypass local minima and to enhance the overall performance a multi-resolution strategy is employed. The associated linear systems are solved via a fast FFT based algorithm,¹⁴ which has a time complexity of $O(N^i \log(N^i))$ where N^i denotes the number of pixels in the image on grid i . The used environment is Matlab 6.5 on a commercially available PC (Pentium 4, 3 GHz, 768 MB RAM).

3.1. An academic example

First we attack the academic example image pair (256×256 pixel) shown in Figure 1a,b. The automatically generated mask for the reference image (figure 5b) nearly coincides with the hand-segmented mask (Figure 5a). Consequently, the registration results (Figure 5c,d) show no significant differences. Both registrations use the parameter set $\alpha = 5$, $\lambda = 1$, $\mu = 100$ and four grid levels with [80, 20, 20, 1] iterations from coarse to fine. The CPU-time for the registration is only 1.78 seconds. To calculate the reference mask the snake algorithm is based on the parameter $\beta = 0.05$, $\gamma = 20$, and $\hat{\mu} = 15$. It does need 20 iterations for computing the GVF vector field and 100 iterations to compute the final mask. The snake schemes consumed about 1.68 seconds, that is, the whole scheme needed less than 4 seconds to compute the final result.

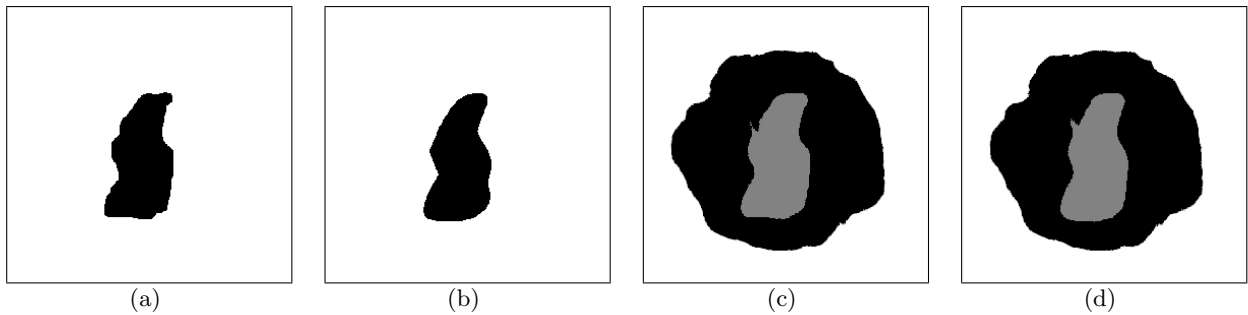


Figure 5. (a) Hand-segmented reference mask, (b) snake based reference mask, (c) registration result based on mask (a), (d) registration result based on mask (b).

3.2. A clinical example

Secondly, we applied our weighted registration method to real-life data. Figure 6 shows the considered abdominal CT images (256×256 pixel) for adaptive radiation therapy planning. The first image (Figure 6a) is taken before the therapy starts. It is used for planning the beam geometry. Before each radiation fraction is applied, a second image (Figure 6b) is taken, which is used for adapting the planned beam geometry to the actual patient position. Since these images are taken days apart, the rectum filling is different, which may cause problems for a registration algorithm. Furthermore, low contrast between different tissue types has to be enhanced in order to guide the registration algorithm.

To perform a weighted elastic registration a reference mask (Figure 6c) and a template mask (Figure 6d) are segmented by hand. The weighting factors are chosen in such a way that the rectum area is suppressed, whereas three low-contrast image areas are enhanced. With these weighting masks, a good registration result (Figure 6f) can be reached, without changing the rectum area. After that, the proposed approach is used to automatically calculate the needed reference mask (Figure 6e). This mask shows some differences compared to the hand-segmented mask (Figure 6c), since edge structures in real images are not as easy to detect as compared to an academic example. Furthermore, finding the rectum mask is complicated by the different fillings, which clearly results in different statistical moments. Nevertheless, the registration result using the automatically generated reference mask (Figure 6g) is comparable to the result with two hand-segmented masks (Figure 6f). Hence, also in this clinical example the automatically chosen reference mask has the same quality as the hand-made one. Both registration schemes use the parameter set $\alpha = 14$, $\lambda = 1$ and $\mu = 4$ with four grid levels with [60, 20, 20, 2]

iterations from coarse to fine. The registration time was about 2.17 seconds. To calculate the reference mask the snake algorithm is started with $\beta = 0.5$, $\gamma = 1$, 100 iterations and $\hat{\mu} = 15$ and 4 iterations for the GVF. It needed about 3.68 seconds. Hence, the real-life example underscore the fact that shows that our method is a very fast alternative (altogether under 6 seconds) to the one with hand-segmented masks.

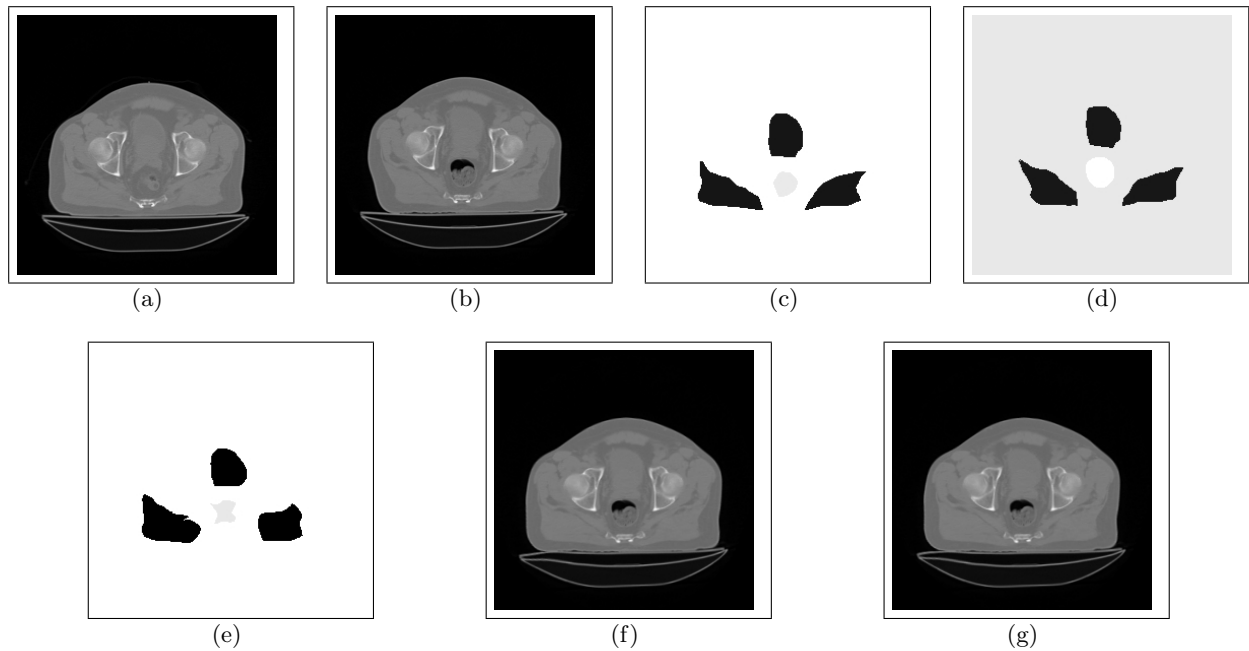


Figure 6. (a) reference, (b) template, (c) hand-segmented reference mask, (d) hand-segmented template mask, (e) snake based reference mask, (f) registration result based on mask (c), (g) registration result based on mask (e). Patient data courtesy of William Beaumont Hospital, Royal Oak, MI.

4. CONCLUSIONS

For a weighted non-parametric registration, a fast method for the calculation of the weighting mask for the reference image is presented. It makes efficiently use of the given template mask and additional pre-knowledge from the template image. A comparison of the results of a registration with the automatically generated reference mask and a weighted registration with two given masks shows a good quality of our new method. Hence computationally expensive segmentation tools are not needed for the reference image. This allows for the use of a weighted registration strategy even in time-critical medical applications. Whenever the template image is recorded long before the reference, the template image can be segmented without time constraints, and the mask for the reference image can be computed “on-the-fly” directly after recording the reference image.

The quality of the registration results achieved with our new approach is the better the better properties of the reference mask can be deduced from the given template mask. As could be seen in the clinical example image, image areas with different contents as for instance different rectum fillings may cause problems since they have different statistical moments and may include irrelevant image edges. Other methods for introducing pre-knowledge into the mask generation process are currently under investigation.

REFERENCES

1. J. Modersitzki, *Numerical methods for image registration*, Oxford University Press, New York, 2003.
2. B. Zitová and J. Flusser, “Image registration methods: A survey,” *Image Vision and Computing* **21**(11), pp. 977–1000, 2003.

3. J. B. A. Maintz and M. A. Viergever, "A survey of medical image registration," *Medical Image Analysis* **2**(1), pp. 1–36, 1998.
4. J. V. Hajnal, D. L. G. Hill, and D. J. Hawkes, *Medical image registration*, CRC Press, Boca Raton.
5. B. Fischer and J. Modersitzki, "Fast diffusion registration," *In AMS Contemporary Mathematics, Inverse Problems, Image Analysis, and Medical Imaging* **313**, pp. 117–129, 2002.
6. R. Bajcsy and Kovačič, "Multiresolution elastic matching," *Computer Vision, Graphics and Image Processing* **46**, pp. 1–21, 1989.
7. C. Broit, *Optimal registration of deformed images*. PhD thesis, Computer and Information Science, University of Pennsylvania, 1981.
8. B. Fischer and J. Modersitzki, "A unified approach to fast image registration and a new curvature based registration technique," *Linear Algebra and its Applications* **380**, pp. 107–124, 2004.
9. P. A. Viola and W. M. Wells III, "Alignment by maximization of mutual information," *Fifth International Conference on Computer Vision, IEEE*, pp. 16–23, 1995.
10. F. Maes, A. Collignon, D. Vandermeulen, G. Marchal, and P. Suetens, "Multimodality image registration by maximization of mutual information," *IEEE Trans Med Imag* **16**, pp. 187–198, 1997.
11. R. C. Gonzales and R. E. Woods, *Digital image processing*, Addison-Wesley, 1993.
12. H. Schumacher, B. Fischer, and A. Franz, "Weighted non-rigid image registration," *submitted*.
13. B. Fischer and J. Modersitzki, "A super fast registration algorithm," in *Bildverarbeitung fuer die Medizin*, M. H. Loew, ed., *Proc. SPIE*, pp. 169–173, (Springer, Luebeck, Germany), 2001.
14. B. Fischer and J. Modersitzki, "Fast inversion of matrices arising in image processing," *Numerical Algorithms* **22**, pp. 1–11, 1999.
15. M. Kass, A. Witkin, and D. Terzopoulos, "Snakes: Active contour models," *Int J Comput Vis* **1**, pp. 321–331, 1987.
16. L. J. Prince and C. Xu, "Snakes, shapes, and gradient vector flow," *IEEE Trans Image Proc* **7**(3).